# On Formulations of Discontinuous Galerkin and Related Methods for Conservation Laws

*H.T. Huynh*
*Glenn Research Center, Cleveland, Ohio*

# NASA STI Program . . . in Profile

Since its founding, NASA has been dedicated to the advancement of aeronautics and space science. The NASA Scientific and Technical Information (STI) program plays a key part in helping NASA maintain this important role.

The NASA STI Program operates under the auspices of the Agency Chief Information Officer. It collects, organizes, provides for archiving, and disseminates NASA's STI. The NASA STI program provides access to the NASA Aeronautics and Space Database and its public interface, the NASA Technical Reports Server, thus providing one of the largest collections of aeronautical and space science STI in the world. Results are published in both non-NASA channels and by NASA in the NASA STI Report Series, which includes the following report types:

- TECHNICAL PUBLICATION. Reports of completed research or a major significant phase of research that present the results of NASA programs and include extensive data or theoretical analysis. Includes compilations of significant scientific and technical data and information deemed to be of continuing reference value. NASA counterpart of peer-reviewed formal professional papers but has less stringent limitations on manuscript length and extent of graphic presentations.

- TECHNICAL MEMORANDUM. Scientific and technical findings that are preliminary or of specialized interest, e.g., quick release reports, working papers, and bibliographies that contain minimal annotation. Does not contain extensive analysis.

- CONTRACTOR REPORT. Scientific and technical findings by NASA-sponsored contractors and grantees.

- CONFERENCE PUBLICATION. Collected papers from scientific and technical conferences, symposia, seminars, or other meetings sponsored or cosponsored by NASA.

- SPECIAL PUBLICATION. Scientific, technical, or historical information from NASA programs, projects, and missions, often concerned with subjects having substantial public interest.

- TECHNICAL TRANSLATION. English-language translations of foreign scientific and technical material pertinent to NASA's mission.

Specialized services also include creating custom thesauri, building customized databases, organizing and publishing research results.

For more information about the NASA STI program, see the following:

- Access the NASA STI program home page at *http://www.sti.nasa.gov*

- E-mail your question to *help@sti.nasa.gov*

- Fax your question to the NASA STI Information Desk at 443–757–5803

- Phone the NASA STI Information Desk at 443–757–5802

- Write to:
  STI Information Desk
  NASA Center for AeroSpace Information
  7115 Standard Drive
  Hanover, MD 21076–1320

# On Formulations of Discontinuous Galerkin and Related Methods for Conservation Laws

*H.T. Huynh*
*Glenn Research Center, Cleveland, Ohio*

National Aeronautics and
Space Administration

Glenn Research Center
Cleveland, Ohio 44135

June 2014

# Acknowledgments

*Level of Review*: This material has been technically reviewed by technical management.

Available from

# On Formulations of Discontinuous Galerkin and Related Methods for Conservation Laws

H.T. Huynh
National Aeronautics and Space Administration
Glenn Research Center
Cleveland, Ohio 44135
huynh@grc.nasa.gov

## Abstract

A formulation for the discontinuous Galerkin (DG) method that leads to solutions using the differential form of the equation (as opposed to the standard integral form) is presented. The formulation includes (a) a derivative calculation that involves only data within each cell with no data interaction among cells, and (b) for each cell, corrections to this derivative that deal with the jumps in fluxes at the cell boundaries and allow data across cells to interact. The derivative with no interaction is obtained by a projection, but for nodal-type methods, evaluating this derivative by interpolation at the nodal points is more economical. The corrections are derived using the approximate (Dirac) delta functions. The formulation results in a family of schemes: different approximate delta functions give rise to different methods. It is shown that the current formulation is essentially equivalent to the flux reconstruction (FR) formulation. Due to the use of approximate delta functions, an energy stability proof simpler than that of Vincent, Castonguay, and Jameson (2011) for a family of schemes is derived. Accuracy and stability of resulting schemes are discussed via Fourier analyses. Similar to FR, the current formulation provides a unifying framework for high-order methods by recovering the DG, spectral difference (SD), and spectral volume (SV) schemes. It also yields stable, accurate, and economical methods.

## 1. Introduction

For conservation laws, e.g., those in the field of Computational Fluid Dynamics (CFD), low-order methods are generally robust and reliable; as a result, they are routinely employed in practical calculations. For the same computing cost, high-order methods can provide considerably more accurate solutions, but they are more complicated and less robust. The need to improve and develop new high-order methods with favorable properties has attracted the interest of many researchers.

The discontinuous Galerkin (DG) method is currently among the most widely used high-order numerical methods for solving conservation laws on unstructured meshes. It was introduced for the neutron transport equation by Reed and Hill (1973), analyzed by LaSaint and Raviart (1974) and developed and made popular for fluid dynamics equations by Cockburn, Shu, Bassi, Rebay, and others (Cockburn, Karniadakis, and Shu 2000, Bassi and Rebay 1997a,b, 2000, Cockburn and Shu 2005, 2009, Shu 2012, and the references therein). Efficient DG schemes storing data at nodal points known as nodal DG methods were elaborated by Hesthaven and Warburton (2008).

Alternative approaches to high-order accuracy employing the differential form (as opposed to DG which employs the integral form) have been proposed. Kopriva and Kolias (1996) pioneered this approach with the staggered-grid spectral method on quadrilateral meshes. The approach was extended to triangular meshes by Liu, Vinokur, and Wang (2006) and named spectral difference (SD), and solutions for a wide range of problems were obtained by Wang et al. (2007) and Liang et al. (2009a and 2009b). Another class of schemes called spectral volume (SV) based on the idea of subdividing each cell into subcells or control volumes in a structured manner was proposed by Wang, Zhang, and Liu (2004).

Recently, an approach to high-order accuracy with the advantage of simplicity and economy called flux reconstruction (FR) was introduced by the author (Huynh 2007, 2009). The approach amounts to evaluating the derivative of a discontinuous piecewise polynomial function by employing its straightforward derivative estimate together with a correction that accounts for the jumps at the interfaces. The FR framework unifies several existing schemes: with appropriate choices of correction terms, it recovers DG, SD, as well as SV, and the FR versions are generally simpler and more economical than the original versions. In addition, the approach results in numerous new methods that are stable and super accurate, i.e., more accurate than expected (also known as super convergent). Extensions of FR to unstructured triangular meshes was provided by Wang and Gao (2009), to the 2D Navier-Stokes equations on meshes of mixed elements by Gao and Wang (2009) and Gao et al. (2013), to the 3D Euler and Navier-Stokes equations on mixed meshes by Haga et al. (2010, 2011) and Wang et al. (2011), and to dynamic meshes by Yu et al. (2012). Whereas FR approach is also known as CPR (Correction Procedure via Reconstruction), due to the usage in references closely related to this work, the name FR is employed.

A mathematical foundation for the FR approach was recently provided by Jameson (2010), who proved that a particular SD scheme (recovered via FR) is energy-stable for 1D linear advection. Vincent, Castonguay, and Jameson (2011a) subsequently extended this result, and proved that a one-parameter family of FR methods is energy-stable for linear advection. This family, referred to as Energy Stable Flux Reconstruction (ESFR), was extended to linear advection on 2D triangular grids by Castonguay, Vincent and Jameson (2012), to linear advection-diffusion in 1D by Castonguay et al. (2013), and to linear advection-diffusion on 2D triangular grids by Williams et al. (2011) and Williams et al. (2013). Von Neumann analyses for these schemes were investigated by Vincent, Castonguay and Jameson (2011b) and nonlinear stability was discussed by Jameson, Vincent and Castonguay (2012). The ESFR methods were shown to be equivalent a filtered DG scheme by Allaneau and Jameson (2012).

A review of recent developments for the FR methods was presented by Huynh, Wang, and Vincent (2014). An open-source Python based framework for solving advection-diffusion type problems on streaming architectures using the FR approach can be found at www.pyfr.org/.

In this paper, a formulation for the discontinuous Galerkin (DG) methods that leads to solutions using the differential form of the equation is presented. The formulation includes (a) a derivative calculation that involves only data within each cell with no data interaction among cells and (b) for each cell, corrections to this derivative that deal with the jumps in fluxes at the cell boundaries and allow data across cells to interact. The derivative with no interaction is obtained by a projection, but for nodal-type methods, evaluating of this derivative by interpolation at the nodal points is more economical. The corrections are derived using the approximate (Dirac) delta functions. The formulation results in a family of schemes: different approximate delta functions give rise to different methods. It is shown that the current formulation is essentially equivalent to the flux reconstruction (FR) formulation. Due to the use of approximate delta functions, an energy stability proof simpler than that of Vincent, Castonguay, and Jameson (2011) for a family of schemes is derived. Accuracy and stability of resulting schemes are discussed via Fourier analyses.

The formulations to be discussed are basic in nature. Therefore, in the hope of attracting the interest of researchers who are not familiar with (some of) these approaches, this paper is written in an essentially self-contained manner. It is organized as follows. The DG method is reviewed in Section 2. Section 3 introduces new strong forms for DG via the use of the approximate Dirac delta functions. The FR schemes, obtained by integrating the strong forms of Section 3, are discussed in Section 4. An energy stability proof for a family of schemes is presented in Section 5. Section 6 contains representative FR schemes and their properties obtained by Fourier analysis. Conclusions and discussion are presented in Section 7. A brief discussion of Fourier stability and accuracy analyses can be found in the Appendix.

# 2. Discontinuous Galerkin Formulations

**2.1. Preliminaries.** Consider the conservation law

$$u_t + f_x = 0 \tag{2.1}$$

with initial condition $u(x, 0) = u_{\text{init}}(x)$. The solution $u$ is assumed to be periodic or of compact support so that boundary conditions are trivial. The flux $f$ depends on $u$. With $a(u) = df/du$, the above can be cast in nonconservation form:

$$u_t + au_x = 0. \tag{2.2}$$

Let the domain of calculation $\Omega$ be divided into possibly nonuniform cells or elements $E_j$, $j = 1, 2, \ldots$ Denote the center of $E_j$ by $x_j$ and its width by $h_j$. Instead of dealing with the global elements, it is more convenient to deal with the local (or reference) element $I = [-1, 1]$. With $\xi$ varying on $I$ and $x$ on $E_j$, the linear function mapping $I$ onto $E_j$ and its inverse are

$$x(\xi) = x_j + \xi h_j/2 \quad \text{and} \quad \xi(x) = 2(x - x_j)/h_j. \tag{2.3}$$

A function $r_j(x)$ on $E_j$ results in a function on $I$ denoted by $r_j(\xi)$ for simplicity of notation, where

$$r_j(\xi) = r_j\big(x(\xi)\big).$$

The derivatives in the global and local descriptions are related by the chain rule

$$\frac{dr_j(x)}{dx} = \left(\frac{2}{h_j}\right)\frac{dr_j(\xi)}{d\xi}. \tag{2.4}$$

For simplicity, when the index is not essential, $E_j$ is denoted by $E$. Let $v$ and $w$ be two functions on $E$; their inner product is given by

$$(v, w)_E = \int_E v(x)w(x) \, dx.$$

The $L^2$ norm of $v$ on $E$ is (a different norm will be discussed later)

$$\|v\|_E = \left(\int_E \big(v(x)\big)^2 \, dx\right)^{1/2}.$$

The inner product in the global description relates to that in the local description by,

$$(v, w)_E = \int_E v(x)w(x) \, dx = \left(\frac{h_j}{2}\right)\int_I v(\xi)w(\xi) \, d\xi = \left(\frac{h_j}{2}\right)(v, w)_I. \tag{2.5}$$

For any nonnegative integer $m$, let $\boldsymbol{P}_m$ be the space of polynomials of degree $m$ or less. The convention $\boldsymbol{P}_m = \{0\}$ for $m < 0$ is also used.

Let the Legendre polynomial $L_m$ be defined as the unique polynomial of degree $m$ that is orthogonal to $\boldsymbol{P}_{m-1}$ and $L_m(1) = 1$. Then, it is well-known (Hildebrandt 1987, Hesthaven and Warburton 2008) that

$$\|L_m\|^2 = (L_m, L_m) = \frac{2}{2m + 1}.$$  (2.6)

**2.2. Discontinuous Galerkin formulations.** Since there are several subtle differences among the various standard and new formulations, for ease of comparison, first, the weak and strong forms of the DG method are re-derived.

Let $k$ be a nonnegative integer. At time $t$, let the solution $u(x, t)$ be approximated on each cell $E_j$ by a polynomial of degree $k$ in $x$ denoted by $u_j(x, t)$. The collection of all $\{u_j(., t)\}$ as $j$ varies forms a function denoted by $u_h$, which is generally discontinuous across cell interfaces. In the reference description for $E = E_j$, with $t$ understood, $u_j$ can be expressed in modal form as

$$u_j(\xi) = \sum_{i=0}^{k} u_{j,i} L_i(\xi).$$  (2.7)

Assume that the data $u_{j,i}(t^n) = u_{j,i}$ are known for all cells. We wish to calculate $\frac{d}{dt} u_{j,i}$ at $t = t^n$.

Note first that since $u_h$ is generally discontinuous across cell interfaces, $f(u_h)$ defined by $f(u_h)(x) = f(u_h(x))$ also shares this property. For the data among cells to interact and, simultaneously, the method to be conservative, we need to define a unique flux for each interface that is common for the two adjacent cells. Also note that, on each cell, $f(u_h)$ can be a non-polynomial function and needs to be approximated as will be discussed later.

Focusing on the cell $E = E_j$, let $\phi$ be a test function, i.e., an element of $\boldsymbol{P}_k$ (independent of $t$). The conservation law (2.1) leads to the following requirement

$$\frac{\partial}{\partial t} (u_h, \phi)_E + \left( (f(u_h))_{x'}, \phi \right)_E = 0.$$  (2.8)

The above relation on $E$, however, involves no interaction with the data of the neighboring cells. To account for data interaction, first, by integration by parts:

$$\frac{\partial}{\partial t} (u_h, \phi)_E + (f(u_h)\phi)_{\partial E} - (f(u_h), \phi_x)_E = 0.$$

For the boundary term $(f(u_h)\phi)_{\partial E}$, at each interface $j + 1/2$, from the left and right $u$ values, namely,

$$u^- = u^-_{j+1/2} = u_j(x_{j+1/2}) \quad \text{and} \quad u^+ = u^+_{j+1/2} = u_{j+1}(x_{j+1/2}),$$  (2.9)

a flux value

$$f^I_{j+1/2} = f^I(u^-, u^+)$$  (2.10)

common for the two adjacent cells $E_j$ and $E_{j+1}$ is employed (the superscript $I$ represents 'interface'). This common flux, also called numerical flux, is typically an upwind-biased flux for advection-type problems. In the case of an advection with constant speed $a$,

$$f^I = \frac{1}{2}a(u^- + u^+) - \frac{1}{2}\beta|a|(u^+ - u^-) \tag{2.11}$$

where $0 \le \beta \le 1$ (with $\beta = 0$ recovering a centered scheme and $\beta = 1$ recovering an upwind scheme). For a diffusion-type problem, the common flux is typically a centered quantity. As for $\phi$, the value from $E$ (no upwinding) is used. For the DG method, the solution is required to satisfy

$$\frac{\partial}{\partial t}(u_h, \phi)_E + (f^I\phi)_{\partial E} - (f(u_h), \phi_x)_E = 0. \tag{2.12}$$

The above is often referred to as the weak form. Denoting the two boundaries of $E$ by the indices $L$ and $R$,

$$\frac{\partial}{\partial t}(u_h, \phi)_E + f_R^I \, \phi_R - f_L^I \, \phi_L - (f(u_h), \phi_x)_E = 0. \tag{2.13}$$

Let the two boundary fluxes using the data inside the cell $E = E_j$ be

$$f_L^+ = f(u_j(x_{j-1/2})) \quad \text{and} \quad f_R^- = f(u_j(x_{j+1/2})). \tag{2.14}$$

Again at the two boundaries of $E$, set

$$[f]_L = f_L^I - f_L^+ \quad \text{and} \quad [f]_R = f_R^I - f_R^-. \tag{2.15}$$

That is, $[f]$ represents the jump or difference between the common interface flux and the flux value just inside the cell (and $[f]_L$ is *not* $f_L^+ - f_L^-$). By applying integration by parts again to (2.12),

$$\frac{\partial}{\partial t}(u_h, \phi)_E + \left((f(u_h))_{x'}, \phi\right)_E + ([f]\phi)_{\partial E} = 0. \tag{2.16}$$

Comparing the above with (2.8), the difference is the boundary term $([f]\phi)_{\partial E}$, which accounts for data interaction. Equivalently,

$$\frac{\partial}{\partial t}(u_h, \phi)_E + \left((f(u_h))_{x'}, \phi\right)_E + [f]_R\phi_R - [f]_L\phi_L = 0. \tag{2.17}$$

Note that the weak and strong forms (2.13) and (2.17) are equivalent if the inner products are carried out exactly. In practice, however, the inner products are approximated by quadrature rules, and the two forms generally produce different results.

## 3. New Strong Forms for the DG Method

The next goal is to rewrite the strong form (2.17) in a manner involving no test function. The formulation below deals with $f_x$ directly and thus differs from the flux reconstruction (FR) formulation, which first reconstructs the flux $f$. As will be shown, the two formulations yield essentially the same schemes with FR typically formulated with the nodal form. The approximate Dirac delta functions below also simplify the energy-stability proof in Section 5.

**3.1. Approximate Dirac delta functions.** These functions are motivated by the boundary terms in (2.17). From here on, unless otherwise stated, inner products take place in the reference frame, i.e., on $I = [-1,1]$. For a fixed $\alpha$ on $I$, let the approximate Dirac delta function at $\alpha$ to degree $k$ be denoted by $\delta_{\alpha,k}$ and defined as the linear functional on $\boldsymbol{P}_k$ that satisfies, for all $\phi$ in $\boldsymbol{P}_k$,

$$\delta_{\alpha,k}(\phi) = \phi(\alpha). \tag{3.1}$$

By a theorem in functional analysis, there exists a member $\gamma_{\alpha,k}$ in $\boldsymbol{P}_k$ such that for all $\phi$ in $\boldsymbol{P}_k$,

$$\left(\gamma_{\alpha,k}, \phi\right) = \delta_{\alpha,k}(\phi) = \phi(\alpha). \tag{3.2}$$

In fact, $\gamma_{\alpha,k}$ can be calculated. First, since it is of degree $k$, it can be expressed as

$$\gamma_{\alpha,k}(\xi) = \sum_{i=0}^{k} b_i\, L_i\,(\xi). \tag{3.3}$$

For any $m \le k$, to obtain $b_m$, apply the dot product with $L_m$ to the above and, using the fact that $L_m$ is orthogonal to all $L_i$, $i \ne m$,

$$\left(\gamma_{\alpha,k}, L_m\right) = b_m(L_m, L_m).$$

By (3.2), $\left(\gamma_{\alpha,k}, L_m\right) = L_m(\alpha)$. This fact together with (2.6) imply

$$L_m(\alpha) = \frac{2}{2m+1} b_m.$$

That is, $b_m = \frac{2m+1}{2} L_m(\alpha)$. Consequently,

$$\gamma_{\alpha,k}(\xi) = \sum_{i=0}^{k} \frac{2i+1}{2} L_i(\alpha)\, L_i\,(\xi). \tag{3.4}$$

See e.g., (Morse and Feshbach 1953, p. 719) where an expression for the Dirac delta function in terms of general eigenvectors can be found.

For simplicity, $\delta_{\alpha,k}$ is considered identical to $\gamma_\alpha$,

$$\delta_\alpha = \delta_{\alpha,k} = \gamma_{\alpha,k} = \gamma_\alpha.$$

Note that for $\alpha = \pm 1$, $|L_i(\alpha)| = 1$; therefore, $L_i(\alpha)^2 = 1$, and

$$\delta_{1,k}(1) = \delta_{-1,k}(-1) = \sum_{i=0}^{k} \frac{2i+1}{2}.$$

As a result,

$$\delta_{1,k}(1) = \delta_{-1,k}(-1) = \frac{(k+1)^2}{2}. \tag{3.5}$$

The above is the maximum value of $\delta_{\pm 1}$ on $I$ and is related to the fact that in conjunction with an explicit time-stepping method, the CFL condition for the DG method is inversely proportional to $(k+1)^2$. In addition, the $i$-th mode of $\delta_{\pm 1}$ satisfies, by (2.6),

$$\left\| \frac{2i+1}{2} L_i(\pm 1) L_i \right\|^2 = \frac{2i+1}{2}.$$

Therefore, after some algebra,

$$\|\delta_{\pm 1}\| = \|\delta_{\pm 1, k}\| = \frac{k+1}{\sqrt{2}}. \tag{3.6}$$

The graphs of $\delta_{0, k}$, $k = 0, 2, 4, 6$, and 8 are shown in Figure 3.1(a). Note that since $L_{2k+1}(0) = 0$, $\delta_{0, 2k+1} = \delta_{0, 2k}$. For comparison, the graphs of $\delta_{1, k}$, $k = 4, \dots, 8$ are shown in Fig. 3.1(b). Note the difference in scales.

**3.2. Strong form S1.** We can now derive the new strong forms. Again unless otherwise stated, we use the local description, and the indices $L$ and $R$ represent $-1$ and $1$, respectively. By (2.4) and (2.5), the strong form (2.17) implies

$$\left( \frac{h_j}{2} \right) (u_h, \phi)_t + \left( (f(u_h))_\xi, \phi \right) + [f]_R \phi_R - [f]_L \phi_L = 0. \tag{3.7}$$

Using (3.4), set

$$\delta_L = \sum_{m=0}^{k} \frac{2i+1}{2} (-1)^i L_i(\xi) \quad \text{and} \quad \delta_R = \sum_{m=0}^{k} \frac{2i+1}{2} L_i(\xi). \tag{3.8a,b}$$

Approx. Dirac delta function at $x = 0$     Approx. Dirac delta function at $x = 1$



(a)     (b)
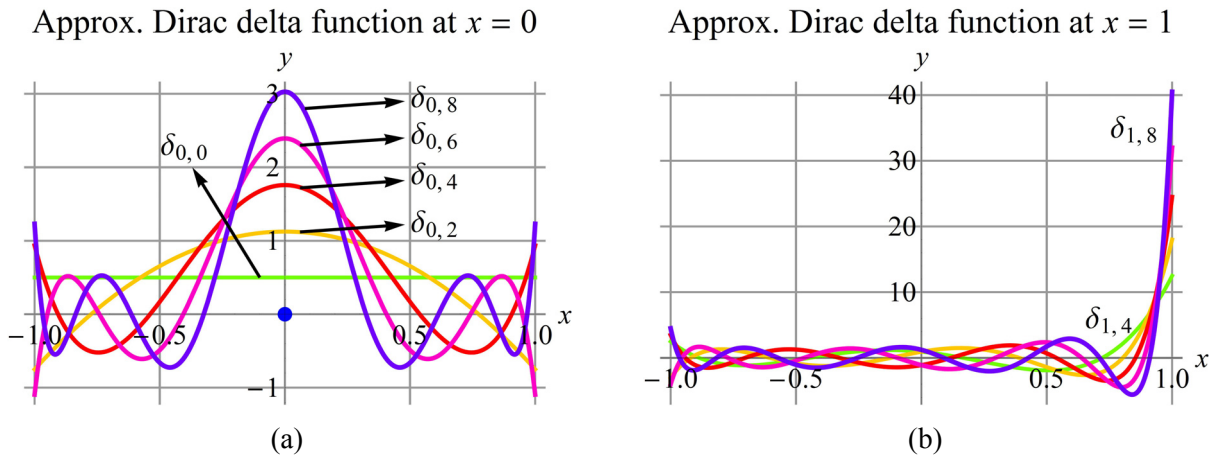
Figure 3.1.—(a) Graphs of $\delta_{0, k}$, $k = 0, 2, 4, 6$, and 8. Since $L_{2k+1}(0) = 0$, $\delta_{0, 2k+1} = \delta_{0, 2k}$. (b) Graphs of $\delta_{1, k}$, $k = 4, 5, \dots, 8$.

Then $\delta_L$ and $\delta_R$ are of degree $k$ and, for all $\phi$ in $\boldsymbol{P}_k$,

$$(\delta_L, \phi) = \phi_L \quad \text{and} \quad (\delta_R, \phi) = \phi_R. \tag{3.9}$$

Thus, (3.7) and the above imply

$$\left(\frac{h_j}{2}\right)(u_h, \phi)_t + \left(\left(f(u_h)\right)_\xi, \phi\right) + [f]_R(\delta_R, \phi) - [f]_L(\delta_L, \phi) = 0. \tag{3.10}$$

For any integer $m \geq 0$, denote by $\mathcal{P}_m$ the projection onto $\boldsymbol{P}_m$, i.e., with any integrable function $v$,

$$\mathcal{P}_m(v) = \sum_{i=0}^{m} \frac{(v, L_i)}{\|L_i\|^2} L_i = \sum_{i=0}^{m} \frac{2i+1}{2} (v, L_i) L_i. \tag{3.11}$$

Due to the fact that $\phi$ is in $\boldsymbol{P}_k$, (3.10) is equivalent to

$$\left(\frac{h_j}{2}\right)(u_h, \phi)_t + \left(\mathcal{P}_k[(f(u_h))_\xi], \phi\right) + [f]_R(\delta_R, \phi) - [f]_L(\delta_L, \phi) = 0. \tag{3.12}$$

The projection $\mathcal{P}_k$ above serves the purpose of cancelling out the test function $\phi$. Indeed, since $u_h$, $\mathcal{P}_k[(f(u_h))_\xi]$, $\delta_R$, and $\delta_L$ are all in $\boldsymbol{P}_k$ and, since $\phi$ spans $\boldsymbol{P}_k$, the above implies the following strong form referred to as S1,

S1 $$\left(\frac{h_j}{2}\right)(u_h)_t + \mathcal{P}_k[(f(u_h))_\xi] + [f]_R\delta_R - [f]_L\delta_L = 0. \tag{3.13}$$

Two remarks concerning the form S1 are in order.

1. Generally, after integrating by parts twice, we get back the original equation. Here, due to the different flux values employed for the boundary terms in each of the two integrations by parts, the strong form S1 looks similar to but not identical with the original conservation laws in the local description. The differences are: (a) the derivative with no interaction is provided by $\mathcal{P}_k[(f(u_h))_\xi]$ and not just $(f(u_h))_\xi$ and (b) the correction for the derivative, namely, $[f]_R\delta_R - [f]_L\delta_L$, provides data interaction among cells and, at the same time, deals with the flux jumps at the interfaces.

2. For numerical algorithms, the interaction of the data among cells involves the functions $\delta_L$ and $\delta_R$, which are derived exactly and are given by (3.8). Concerning $\mathcal{P}_k[(f(u_h))_\xi]$, which represents the derivative with no interaction, $u_h$ is in $\boldsymbol{P}_k$, but $f(u_h)$ needs not be a polynomial in general. For nodal-type schemes, $\mathcal{P}_k[(f(u_h))_\xi]$ can be approximated conveniently and effectively by using the chain rule at the nodal points $\xi_i$, $i = 0, \dots, k$: $\left(f(u_h)\right)_\xi(\xi_i) = a\big(u_h(\xi_i)\big)(u_h)_\xi(\xi_i)$.

3. The strong form (3.13) leads to a family of schemes by altering the criteria of approximation for the Dirac delta function. What is crucial is that the resulting scheme must be stable and accurate.

**3.3. Strong form S2.** We next present an alternative to the strong form S1. Concerning again the derivative with no interaction, we can first approximate $f(u_h)$ by its projection $\mathcal{P}_k(f(u_h))$ and then calculate the derivative: the result is referred to as S2,

S2
$$\left(\frac{h_j}{2}\right)(u_h)_t + [\mathcal{P}_k(f(u_h)]_\xi + [f]_R\delta_R - [f]_L\delta_L = 0. \tag{3.14}$$

For this strong form, the two boundary fluxes interior to cell $E = E_j$ are defined as, instead of (2.14),

$$f_L^+ = [\mathcal{P}_k(f(u_j))](x_{j-1/2}) \quad \text{and} \quad f_R^- = [\mathcal{P}_k(f(u_j))](x_{j+1/2}) \tag{3.15}$$

and the jumps $[f]$ at the two interfaces are defined using the above interior values.

The following remarks are in order.

1. For this strong form, similar to the case of S1, concerning the derivative with no interaction $[\mathcal{P}_k(f(u_h)]_\xi$, with nodal-type schemes, we can first approximate $f(u_h)$ by its values at the nodal points and then evaluate the derivative of the resulting polynomial. Such an approximation is said to be via 'Lagrange polynomial' whereas that in the second remark after (3.13) is via 'chain rule'. These two ways of approximating the derivative with no interaction were mentioned by the author as alternative approaches (Huynh 2007). Later, Wang and Gao (2009) found that for nonlinear problems such as the Euler equations, the solution via the chain rule was more accurate.

2. With the current strong forms S1 and S2, the conservation law for nodal-type methods is solved via a combination of interpolation and projection: the derivative with no interaction is approximated via interpolation, and the two boundary corrections are carried out exactly to degree $k$ via projection since the approximate Dirac delta functions $\delta_{\pm 1}$ are exact up to degree $k$. The evaluation of $\delta_{\pm 1}(\xi)$ at the nodes incurs no additional (interpolation) errors. Also note that the approximation to the derivative with no interaction $(f(u_h))_\xi$ can be carried out via projection as well but, typically, projection for such a function is costlier than interpolation; moreover, projection is typically approximated by a quadrature which, similar to interpolation, incurs errors.

3. For the case of advection with constant speed, the strong forms S1 and S2 become identical and is called strong form S. The reason is that since $f(u_j) = au_j$ is of degree $k$, both approaches for the derivative with no interaction result in $a(u_j)_\xi$, which is of degree $k-1$. In the general case of nonlinear conservation laws, however, the two forms are different: the polynomial $[\mathcal{P}_k(f(u_h)]_\xi$ for S2 is of degree $k-1$ as opposed to $\mathcal{P}_k[(f(u_h))_\xi]$ for S1, which is of degree $k$. The lower degree approximation of S2 appears to be consistent with the numerical findings of Wang and Gao (2009) mentioned above.

4. The key difference between the current strong forms and a standard DG strong form such as (2.17) is that by employing the approximate Dirac delta functions, the current ones involve no test functions. As will be shown, they also unify existing methods by recovering the spectral difference schemes via an appropriate modification to the approximate Dirac delta function; in addition, these strong forms result in a family of energy-stable methods that have the property of super accuracy (i.e., more accurate than expected via Fourier analysis as discussed by Huynh (2007) and Vincent et al. (2011)).

**3.4. Conservation property.** Next, we show that the strong form S1 is conservative, i.e.,

$$\frac{\partial}{\partial t}\int_E u_h(x)\,dx = f_L^I - f_R^I. \tag{3.16}$$

Note first that for any integrable function $w$ on $I$, the projection preserves the cell average quantity,

$$\int_{-1}^{1} \mathcal{P}_k(w) \, d\xi = \int_{-1}^{1} w \, d\xi. \tag{3.17}$$

Therefore, with $v_\xi = w$,

$$\int_{-1}^{1} \mathcal{P}_k(v_\xi) \, d\xi = \int_{-1}^{1} v_\xi \, d\xi = v(1) - v(-1). \tag{3.18}$$

Applying the above to $\mathcal{P}_k[(f(u_h))_\xi]$, we obtain

$$\int_{-1}^{1} \mathcal{P}_k[(f(u_h))_\xi] \, d\xi = \int_{-1}^{1} (f(u_h))_\xi \, d\xi = f_R^- - f_L^+ \tag{3.19}$$

where $f_L^+$ and $f_R^-$ are the boundary fluxes interior to $E$ as defined in (2.14). Next, for the cell $E_j$, in the local description, (3.12) with $\phi = 1$ implies

$$\left(\frac{h_j}{2}\right) \frac{\partial}{\partial t} \int_{-1}^{1} u_j \, d\xi + \int_{-1}^{1} \mathcal{P}_k[(f(u_j))_\xi] \, d\xi + [f]_R - [f]_L = 0. \tag{3.20}$$

By (3.23) and (2.15), Eq. (3.20) follows. This completes the proof.

The conservative property of the scheme S2 is similar with (3.15) replacing (2.14) and, therefore, omitted.

A modification to assure conservation property when using the derivative with no interaction via the chain rule on 2D unstructured meshes was provided by Gao and Wang (2013).

## 4. DG Scheme Via Flux Reconstruction (FR) Approach

We now present a formulation which deals with $f$ rather than $f_x$ as in the previous section. It will be shown that for the DG method, the slope $f_x$ for the conservation law is given by $(F_j)_x$ where, on each cell $E_j$, $F_j$ is a polynomial of degree $k + 1$ defined by (a) $F_j$ takes on the common interface flux values at the two cell boundaries and (b) $\mathcal{P}_{k-1}(F_j) = \mathcal{P}_{k-1}(f(u_h))$. The key idea here for constructing $F_j$ is to integrate the strong form S1.

**4.1. Approximating the flux $f(u_h)$ with no interaction.** In the form S1, the derivative with no interaction is approximated by $\mathcal{P}_k[(f(u_h))_\xi]$. This approximation is equivalent to a certain approximation for the flux $f$ itself. In what manner is $f$ approximated?

To answer the above question, first, by the fundamental theorem of Calculus,

$$(f(u_h))(\eta) = f_L^+ + \int_{-1}^{\eta} (f(u_h))_\xi \, d\xi. \tag{4.1}$$

Next, with subscript IPD short for 'integrating the projection of the derivative', set

$$f_{\text{IPD}}(\eta) = f_L^+ + \int_{-1}^{\eta} \mathcal{P}_k[(f(u_h))_\xi] \, d\xi. \tag{4.2}$$

Then $f_{\mathrm{IPD}}$ is of degree $k + 1$ and, the second equation below is due to (3.19),

$$f_{\mathrm{IPD}}(-1) = f_L^+ \quad \text{and} \quad f_{\mathrm{IPD}}(1) = f_R^-. \tag{4.3}$$

That is, $f_{\mathrm{IPD}}$ interpolates $f(u_h)$ at the two cell boundaries. Two conditions for $f_{\mathrm{IPD}}$ are known, $k$ conditions remain to describe how it approximates $f(u_h)$.

To obtain these remaining conditions, let $\phi$ be in $\boldsymbol{P}_k$. Integration by parts yields

$$\left(f_{\mathrm{IPD}}, \phi_\xi\right) = f_R^- \phi_R - f_L^+ \phi_L - \left((f_{\mathrm{IPD}})_\xi, \phi\right). \tag{4.4}$$

By (4.2), $(f_{\mathrm{IPD}})_\xi = \mathcal{P}_k[(f(u_h))_\xi]$. Thus, the above implies

$$\left(f_{\mathrm{IPD}}, \phi_\xi\right) = f_R^- \phi_R - f_L^+ \phi_L - \left(\mathcal{P}_k[(f(u_h))_\xi], \phi\right). \tag{4.5}$$

Next, in (4.5), since $\phi$ is in $\boldsymbol{P}_k$, we can replace $\mathcal{P}_k[(f(u_h))_\xi]$ by $(f(u_h))_\xi$, and since $\phi_\xi$ is in $\boldsymbol{P}_{k-1}$, we can replace $f_{\mathrm{IPD}}$ by $\mathcal{P}_{k-1}(f_{\mathrm{IPD}})$,

$$\left(\mathcal{P}_{k-1}(f_{\mathrm{IPD}}), \phi_\xi\right) = f_R^- \phi_R - f_L^+ \phi_L - \left((f(u_h))_\xi, \phi\right). \tag{4.6}$$

By applying integration by parts to the inner product of the right hand side,

$$\left(\mathcal{P}_{k-1}(f_{\mathrm{IPD}}), \phi_\xi\right) = \left((f(u_h)), \phi_\xi\right). \tag{4.7}$$

As $\phi$ spans $\boldsymbol{P}_k$, $\phi_\xi$ spans $\boldsymbol{P}_{k-1}$; therefore, the above implies

$$\mathcal{P}_{k-1}(f_{\mathrm{IPD}}) = \mathcal{P}_{k-1}(f(u_h)). \tag{4.8}$$

Thus, in the strong form S1, $\mathcal{P}_k[(f(u_h))_\xi]$ approximates $(f(u_h))_\xi$ in the sense of projection by its definition. Equivalently, its integral $f_{\mathrm{IPD}}$ defined by (4.2), which is a polynomial of degree $k + 1$, approximates $f(u_h)$ in the sense of a combination of interpolation at the two boundaries as in (4.3), and projection as above.

**4.2. Correction functions.** We now deal with the boundary terms of the form S1 or (3.13). With $\delta_R$ by (3.8b), let the correction function for the right boundary be denoted by $g_{R,DG}$ or simply $g_R$ and defined by

$$g_R(\xi) = \int_{-1}^{\xi} \delta_R(\eta) d\eta. \tag{4.9}$$

(In Section 6, $g_R$ denotes the correction function for a more general scheme, not just DG.) Then, $g_R$ is of degree $k + 1$ and

$$g_R' = \delta_R. \tag{4.10}$$

Moreover,

$$g_R(-1) = 0 \quad \text{and} \quad g_R(1) = 1, \tag{4.11a,b}$$

where the second equation results from (4.9) with $\xi = 1$ together with (3.2) where $\phi = 1$. Note that since $\delta_R$ approximates the Dirac delta function at $\xi = 1$, $g_R$ approximates the Heaviside or unit step (step up) function at the same location.

Next, it is shown that

$$\mathcal{P}_{k-1}(g_R) = 0. \tag{4.12}$$

Indeed, by integration by parts, for any polynomial $v$ of degree $k$,

$$(g_R, v') = v(1) - \int_{-1}^{1} g_R'(\xi)v(\xi)d\xi = v(1) - \int_{-1}^{1} \delta_R(\xi)v(\xi)d\xi = 0. \tag{4.13}$$

As $v$ spans $\boldsymbol{P}_k$, $v'$ spans $\boldsymbol{P}_{k-1}$; therefore, (4.12) holds.

Let the correction function for the left boundary be defined by (note the change in the integration limits)

$$g_L(\xi) = \int_{\xi}^{1} \delta_L(\eta)d\eta. \tag{4.14}$$

(Again a more precise notation is $g_{L,DG}$; however, the subscript DG is understood in this section.) Then, $g_L$ is of degree $k + 1$ and

$$g_L' = -\delta_L. \tag{4.15}$$

Moreover,

$$g_L(-1) = 1 \quad \text{and} \quad g_L(1) = 0, \tag{4.16a,b}$$

where the first equation results from (4.14) with $\xi = -1$ together with (3.2) where $\phi = 1$. Note that since $\delta_L$ approximates the Dirac delta function at $\xi = -1$, $g_L$ approximates the step down function which takes on the value 1 at $\xi = -1$ and the value 0 for $-1 < \xi \leq 1$.

In addition,

$$\mathcal{P}_{k-1}(g_L) = 0. \tag{4.17}$$

The proof is similar to that of (4.12) and is omitted.

**4.3. Flux reconstruction.** The reconstruction of the flux on $E = E_j$ can now be carried out. At the two interfaces, recall that $f_L^+ = f(u_j(-1))$, $f_R^- = f(u_j(1))$, $[f]_L = f_L^I - f_L^+$, and $[f]_R = f_R^I - f_R^-$.

From Subsection 4.1 above, $f_{\text{IPD}}$ is of degree $k + 1$, involves no interaction among cells, takes on the values $f_L^+$ and $f_R^-$ at the left and right interfaces, respectively, and $\mathcal{P}_{k-1}(f_{\text{IPD}}) = \mathcal{P}_{k-1}(f(u_h))$. Next, the function

$$f_{\text{IPD}} + [f]_L \, g_L$$

recovers the common flux value at the left interface, namely $f_{j-1/2}^I$, due to the condition $g_L(-1) = 1$. It's value at the right interface is unchanged from that of $f_{\text{IPD}}$, namely the value $f_R^-$; this is due to the condition $g_L(1) = 0$. The function

$$F_j = f_{\text{IPD}} + [f]_L\, g_L + [f]_R\, g_R \tag{4.18}$$

takes on the common interface flux values at the two boundaries,

$$F_j(-1) = f_L^I \quad \text{and} \quad F_j(1) = f_R^I. \tag{4.19}$$

In addition, on $E_j$, by (4.8), (4.12), and (4.17),

$$\mathcal{P}_{k-1}(F_j) = \mathcal{P}_{k-1}(f(u_j)). \tag{4.20}$$

Finally, by (4.2), (4.10), and (4.15), Eq. (4.18) implies

$$F_j' = \mathcal{P}_k[(f(u_h))_\xi] - [f]_L\delta_L + [f]_R\delta_R. \tag{4.21}$$

Note that the above right hand side is identical to that of the strong form S1 of (3.13). This completes the derivation of DG schemes via FR approach.

A few remarks are in order.

1. Due to (4.19), the collection of all $\{F_j\}$ as $j$ varies forms a function which is continuous across cell interfaces, and $F_j'$ yields the DG approximation for $f_x$ for the conservation law.

2. The flux reconstruction form (4.18) above leads to a family of schemes by using different criteria to define the correction function $g_L$ and $g_R$. What is crucial is that the criteria must result in stable and accurate methods.

3. In the weak form (2.13) for the DG scheme, $f(u_h)$ can be replaced by $\mathcal{P}_{k-1}(f(u_h))$ since $\phi_x$ is of degree $k - 1$,

$$\frac{\partial}{\partial t}(u_h, \phi)_E + f_R^I\, \phi_R - f_L^I\, \phi_L - (\mathcal{P}_{k-1}(f(u_h)), \phi_x)_E = 0. \tag{4.22}$$

Thus, due to (4.19) and (4.20), the definition for $F_j$ by (4.18) is, loosely put, consistent with the weak form above.

## 5. Energy Stable Flux Reconstruction Schemes (ESFR)

Energy stability for a family of schemes can now be shown. Consider the case of advection with constant speed $a \geq 0$ (the wind blows from left to right). We also assume that the initial data is periodic or of compact support so that boundary conditions are trivial.

**5.1. Energy stability of the DG scheme.** First, it is well-known that the DG scheme with the upwind biased flux (2.11) is energy stable. The simple proof, which can be found in (Jameson 2011), plays a critical role below; therefore, it is included.

The strong form (2.17) on $E = E_j$ with $\phi = u_j$ implies

$$\left(\frac{\partial}{\partial t}u_j, u_j\right)_E + \left\{\left(a\left(u_j\right)_x, u_j\right)_E + (f_{j+1/2}^I - f_{j+1/2}^-)u_{j+1/2}^- - (f_{j-1/2}^I - f_{j-1/2}^+)u_{j-1/2}^+\right\} = 0. \quad (5.1)$$

Note that $\left(a(u_j)_\xi, u_j\right) = \frac{a}{2}\left[\left(u_{j+1/2}^-\right)^2 - \left(u_{j-1/2}^+\right)^2\right]$. With $f_{j+1/2}^I = au_{j+1/2}^I$ for each interface, the expression in the curly bracket above can be written as

$$a(u_{j+1/2}^I - \tfrac{1}{2}u_{j+1/2}^-)u_{j+1/2}^- - a(u_{j-1/2}^I - \tfrac{1}{2}u_{j-1/2}^+)u_{j-1/2}^+. \quad (5.2)$$

At each interface $j - 1/2$, collecting the contributions from the element $E_{j-1}$ and then $E_j$, there is a total contribution of

$$a(u_{j-1/2}^I - \tfrac{1}{2}u_{j-1/2}^-)u_{j-1/2}^- - a(u_{j-1/2}^I - \tfrac{1}{2}u_{j-1/2}^+)u_{j-1/2}^+. \quad (5.3)$$

Omitting the subscript $j - 1/2$, we obtain $a[(u^I - \tfrac{1}{2}u^-)u^- - (u^I - \tfrac{1}{2}u^+)u^+]$. After some algebra, and using the upwind-biased flux (2.11), the result is

$$\tfrac{1}{2}\beta|a|(u^+ - u^-)^2. \quad (5.4)$$

Recall that $0 \le \beta \le 1$. Thus, on the whole physical domain, with our periodic or of compact support assumption for the data, (5.1) and the above imply

$$\frac{1}{2}\frac{\partial}{\partial t}\int_\Omega u_h^2 \, dx = -\sum_j \frac{1}{2}\beta|a|\left(u_{j-1/2}^+ - u_{j-1/2}^-\right)^2 \le 0. \quad (5.5)$$

That is, energy of the numerical solution can only decrease in time. This completes the proof that the DG scheme in semi-discrete form using the upwind-biased common flux is energy stable for the linear advection equation.

What we need from the above proof is the fact that the quantity in the square bracket of (5.1) implies (5.4) at each interface after the square bracket quantities from the two adjacent cells are collected.

**5.2. Energy stability of a family of FR scheme.** For the current case of advection, as discussed in the third remark after (3.15), the two strong forms S1 and S2 become identical and are referred to as strong form S. On $E_j$, set

$$f_j = f\left(u_j\right) = au_j. \quad (5.6)$$

To obtain a family of schemes, we replace $\delta$ in the strong form S of (3.13) by $\delta + \epsilon$, where $\epsilon$ provides the variation:

$$\left(\frac{h_j}{2}\right)(u_j)_t + (f_j)_\xi - [f]_L(\delta_L + \epsilon_L) + [f]_R(\delta_R + \epsilon_R) = 0. \quad (5.7)$$

In other words, we approximate the Dirac delta function not by $\delta$ but by $\delta + \epsilon$, which results in a family of schemes. What is crucial is that $\epsilon$ must be chosen in a manner that the resulting scheme is stable and accurate. In this section, we assume $\epsilon$ involves only the highest mode:

$$\epsilon_L = (-1)^k \epsilon_k L_k \quad \text{and} \quad \epsilon_R = \epsilon_k L_k. \tag{5.8a,b}$$

The coefficient $(-1)^k$ above is for being consistent with (3.8a). We wish to show that if

$$\epsilon_k > -\frac{2k+1}{2}, \tag{5.9}$$

then the resulting scheme is energy-stable *under a certain energy norm* to be defined later.

Compared with the coefficient of the highest mode of $\delta_R$ which, by (3.8b), equals $\frac{2k+1}{2}$, the above condition is equivalent to the fact that the highest mode of $\delta_R + \epsilon_R$ has a strictly positive coefficient, i.e.,

$$\delta_R + \epsilon_R = \alpha_k L_k + \sum_{i=0}^{k-1} \frac{2i+1}{2} L_i = \alpha_k L_k + \delta_{R,k-1}. \tag{5.10}$$

where

$$\alpha_k = \frac{2k+1}{2} + \epsilon_k > 0. \tag{5.11}$$

For the left boundary,

$$\delta_L + \epsilon_L = (-1)^k \alpha_k L_k + \delta_{L,k-1}. \tag{5.12}$$

The following proof is similar to but simpler than that of Vincent et al. (2011) due to the use of the approximate Dirac delta functions.

Using technique employed in (5.1), multiplying (5.7) by $u_j$ and integrating on $I$, we obtain

$$\frac{h_j}{4} \frac{d}{dt} \int_{-1}^{1} u_j^2 \, d\xi = -\int_{-1}^{1} u_j (f_j)_\xi \, d\xi + [f]_L u_{j,L} - [f]_R u_{j,R} +$$
$$[f]_L \int_{-1}^{1} u_j \epsilon_L \, d\xi - [f]_R \int_{-1}^{1} u_j \epsilon_R \, d\xi. \tag{5.13}$$

Set

$$R = [f]_L \int_{-1}^{1} u_j \epsilon_L \, d\xi - [f]_R \int_{-1}^{1} u_j \epsilon_R \, d\xi. \tag{5.14}$$

Eq. (5.13) implies

$$\frac{h_j}{4} \frac{d}{dt} \int_{-1}^{1} u_j^2 \, d\xi - R = -\left\{ \int_{-1}^{1} u_j (f_j)_\xi \, d\xi - [f]_L u_{j,L} + [f]_R u_{j,R} \right\}. \tag{5.15}$$

The square bracket quantity above equals the square bracket quantity in (5.1), which will result in (5.4) at the interfaces.

We now derive conditions on $\epsilon_k$ so that the above left hand side results in the time rate of change of a certain energy norm. Our goal is to relate $R$ of (5.14), which does not involve $\frac{d}{dt}$, with $\frac{d}{dt}\left(u_{j,k}^2(t)\right)$ where $u_{j,k}^2$ is, up to a constant factor, the energy of the $k$-th mode of $u_j$.

To this end, first, on $I$,

$$\|u_j\|^2 = \int_{-1}^{1} u_j^2 \, d\xi = \sum_{i=0}^{k} u_{j,i}^2(L_i, L_i) = \sum_{i=0}^{k} \frac{2}{2i+1} u_{j,i}^2. \tag{5.16}$$

Next, since $\epsilon_L$ and $\epsilon_R$ involve only the highest mode as expressed in (5.8), and since the $k$-th mode of $u_j$ is $u_{j,k}L_k$, Eq. (5.14) implies

$$R = \epsilon_k \, u_{j,k} \, \|L_k\|^2 \left\{ (-1)^k [f]_L - [f]_R \right\}. \tag{5.17}$$

Following (Jameson 2010) and (Vincent et al. 2011), differentiate (5.7) $k$ times (in space),

$$\frac{h_j}{2} \frac{\partial}{\partial t} \frac{\partial^k u_j}{\partial \xi^k} + \frac{\partial^{k+1} f_j}{\partial \xi^{k+1}} - [f]_L \frac{\partial^k (\delta_L + \epsilon_L)}{\partial \xi^k} + [f]_R \frac{\partial^k (\delta_R + \epsilon_R)}{\partial \xi^k} = 0. \tag{5.18}$$

Since $f_j$ is of degree $k$,

$$\frac{\partial^{k+1} f_j}{\partial \xi^{k+1}} = 0. \tag{5.19}$$

Multiplying (5.18) by $\frac{\partial^k u_j}{\partial \xi^k}$,

$$\frac{h_j}{4} \frac{\partial}{\partial t} \left(\frac{\partial^k u_j}{\partial \xi^k}\right)^2 - [f]_L \frac{\partial^k u_j}{\partial \xi^k} \frac{\partial^k (\delta_L + \epsilon_L)}{\partial \xi^k} + [f]_R \frac{\partial^k u_j}{\partial \xi^k} \frac{\partial^k (\delta_R + \epsilon_R)}{\partial \xi^k} = 0. \tag{5.20}$$

Integrating on $I$, we obtain

$$\frac{h_j}{4} \frac{d}{dt} \int_{-1}^{1} \left(\frac{\partial^k u_j}{\partial \xi^k}\right)^2 d\xi = \tilde{R} \tag{5.21}$$

where

$$\tilde{R} = [f]_L \int_{-1}^{1} \frac{\partial^k u_j}{\partial \xi^k} \frac{\partial^k (\delta_L + \epsilon_L)}{\partial \xi^k} d\xi - [f]_R \int_{-1}^{1} \frac{\partial^k u_j}{\partial \xi^k} \frac{\partial^k (\delta_R + \epsilon_R)}{\partial \xi^k} d\xi. \tag{5.22}$$

For the left hand side of (5.21), denote

$$m_k = \frac{\partial^k L_k}{\partial \xi^k}.$$

Then, $m_k$ is a constant. In fact, $m_k = k! \, a_k = (2k-1)!/(2^{k-1}(k-1)!)$ where $a_k$ is the leading coefficient of $L_k$; however, this expression is not essential. Concerning the left hand side of (5.21),

$$\frac{\partial^k u_j}{\partial \xi^k} = u_{j,k} \qquad \frac{\partial^k L_k}{\partial \xi^k} = u_{j,k}\, m_k. \tag{5.23}$$

Consequently, recalling that $u_{j,k} = u_{j,k}(t)$, the left hand side of (5.21) equals $\frac{h_j}{2}\frac{d}{dt}\left(m_k^2\, u_{j,k}^2\right)$ where we use the fact that $\int_{-1}^1 1\, d\xi = 2$. That is, (5.21) can be written as

$$\frac{h_j}{4}\frac{d}{dt}\int_{-1}^1 \left(\frac{\partial^k u_j}{\partial \xi^k}\right)^2 d\xi = \frac{h_j}{2}\frac{d}{dt}\left(m_k^2\, u_{j,k}^2\right) = \tilde{R}. \tag{5.24}$$

We now relate $\tilde{R}$ defined by (5.22) with $R$ of (5.17). The key fact employed is that $\tilde{R}$ involves only the highest mode. First, by (3.8a) for $\delta_L$ and (5.8a) for $\epsilon_L$,

$$\frac{\partial^k(\delta_L + \epsilon_L)}{\partial \xi^k} = (-1)^k \left(\frac{2k+1}{2} + \epsilon_k\right) m_k,$$

and by (3.8b) for $\delta_R$ and (5.8b) for $\epsilon_R$,

$$\frac{\partial^k(\delta_R + \epsilon_R)}{\partial \xi^k} = \left(\frac{2k+1}{2} + \epsilon_k\right) m_k.$$

Due to the above two expressions and (5.23), Eq. (5.22) implies

$$\tilde{R} = (2k+1+2\epsilon_k)\, m_k^2\, u_{j,k} \left\{ (-1)^k [f]_L - [f]_R \right\} \tag{5.25}$$

Using the above and the fact that $\|L_k\|^2 = 2/(2k+1)$, Eq. (5.17) implies

$$R = \frac{2\epsilon_k}{(2k+1)(2k+1+2\epsilon_k)m_k^2}\, \tilde{R}. \tag{5.26}$$

Thus, by (5.24),

$$R = \frac{\epsilon_k}{(2k+1)(2k+1+2\epsilon_k)}\, h_j\, \frac{d(u_{j,k}^2)}{dt}. \tag{5.27}$$

What is crucial is that $R$ of (5.14), which involves no time derivative, can be expressed as above, which involves the time derivative and the highest component $u_{j,k}$.

By the above, the left hand side of (5.15) yields

$$\frac{h_j}{4}\frac{d}{dt}\int_{-1}^1 u_j^2\, d\xi - R = \frac{h_j}{4}\frac{d}{dt}\left\{\int_{-1}^1 u_j^2\, d\xi - \frac{4\epsilon_k}{(2k+1)(2k+1+2\epsilon_k)}\, u_{j,k}^2\right\}. \tag{5.28}$$

Using (5.16), the $k$-th mode of the above right hand side equals

$$\frac{h_j}{4}\frac{d}{dt}\left\{\left[1 - \frac{2\epsilon_k}{(2k+1+2\epsilon_k)}\right]\frac{2}{2k+1}\, u_{j,k}^2\right\}. \tag{5.29}$$

For the above to result in a norm, it is required that

$$1 - \frac{2\epsilon_k}{(2k + 1 + 2\epsilon_k)} > 0 \tag{5.30}$$

or, $(2k + 1 + 2\epsilon_k - 2\epsilon_k)/(2k + 1 + 2\epsilon_k) > 0$ or $(2k + 1)/(2k + 1 + 2\epsilon_k) > 0$ or $(2k + 1 + 2\epsilon_k) > 0$, or

$$\epsilon_k > -\frac{2k + 1}{2}. \tag{5.31}$$

Thus, instead of the standard norm (5.16), we employ a modified energy norm on $E = E_j$ defined by

$$\|u_j\|_M^2 = \frac{h_j}{2}\left[\left(1 - \frac{2\epsilon_k}{(2k + 1 + 2\epsilon_k)}\right)\frac{2}{2k + 1}u_{j,k}^2 + \sum_{i=0}^{k-1}\frac{2}{2i + 1}u_{j,i}^2\right]. \tag{5.32}$$

Or, equivalently, by (5.23),

$$\|u_j\|_M^2 = = \frac{h_j}{2}\left[\int_{-1}^{1}u_j^2\,d\xi - \frac{2\epsilon_k}{(2k + 1 + 2\epsilon_k)(2k + 1)m_k^2}\int_{-1}^{1}\left(\frac{\partial^k u_j}{\partial\xi^k}\right)^2 d\xi\right]. \tag{5.33}$$

Thus, using the above norm, the family of schemes via the approximate Dirac delta function of $\delta + \epsilon$, where the highest mode of $\delta_R + \epsilon_R = \alpha_k L_k + \delta_{R,k-1}$ has a strictly positive coefficient $\alpha_k$, is energy stable. This completes the energy-stability proof.

The following three remarks are in order.

1. The energy-stability proof of Vincent et al. (2011) was extended to nonlinear conservation laws in Jameson, Vincent, and Castonguay (2012). There, it was also shown that similar to DG, the FR methods may encounter aliasing driven instability if the flux function is non-linear. They demonstrated that for nodal methods, the location of the solution points plays an important role in determining the extent of aliasing driven instabilities, and the strong quadrature points such as Gauss points are optimal in minimizing such instabilities.

2. The energy-stability proof here also extends to nonlinear conservation laws provided that (a) the strong form S2 is employed and (b) the interface flux is an E-flux (Osher 1984, Jiang and Shu 1994); this extension is similar to that by Jameson, Vincent, and Castonguay (2012) mentioned above.

3. It remains an open problem to prove or disprove that for the strong form S1, in the case of nonlinear conservation laws, the family of schemes discussed here is stable. The above proof does *not* extend for the following reason. A key ingredient of the proof is condition (5.19) or $\partial^{k+1}f_j/\partial\xi^{k+1} = 0$. For the strong form S1 of (3.13), the quantity $\partial^{k+1}f_j/\partial\xi^{k+1}$ is replaced by $\partial^k(\mathcal{P}_k[(f(u_h))_\xi])/\partial\xi^k$, which may not vanish. Also note that for nonlinear conservation laws and the strong form S1, whereas the stability of the family of schemes is not known, the stability for DG using the weak form (and thus the strong form S1) is well established as discussed in (Jiang and Shu 1994).

## 6. Flux Reconstruction/Correction Procedure via Reconstruction (FR/CPR) Schemes

The FR methods, which are obtained by different criteria of approximation for the (Dirac) delta function in the strong form S1, or different definitions for the correction functions in constructing $F_j$ via (4.18), are discussed in this section. Their accuracy and stability properties by Fourier analyses are also

mentioned. The current presentation of these methods provides additional relations not available in the literature.

Focusing on the right boundary, recall that in the case of the DG scheme, the correction function $g_{R,DG}$ is of degree $k+1$ and defined by the $k+2$ conditions of $g_{R,DG}(-1) = 0$, $g_{R,DG}(1) = 1$, and $\mathcal{P}_{k-1}(g_{R,DG}) = 0$ of (4.12). Its derivative is the approximate delta function $\delta_R = \delta_{R,k}$ given in (3.8b).

To obtain a family of schemes, the correction function $g_R$ of degree $k+1$ is required to satisfy

$$g_R(-1) = 0, \quad g_R(1) = 1, \tag{6.1a,b}$$

together with $k$ additional conditions. As discussed before (4.18), when reconstructing the flux, the condition $g_R(1) = 1$ serves the purpose of recovering the common flux value $f^I_{j+1/2}$ at the right interface whereas condition $g_R(-1) = 0$ leaves the value at the left interface unchanged. The $k$ additional conditions correspond to the fact that $g_R$ approximates the zero function on $[-1, 1)$ (consistent with the remark after (4.11) that $g_R$ approximates the unit step function) in some sense. These approximation criteria must be chosen in a manner that the corresponding scheme is stable and accurate.

**6.1. Radau and Lobatto polynomials and their derivatives.** The following polynomials play an important role in the definitions of various correction functions and their derivatives.

**Radau polynomials.** Let the left Radau polynomial of degree $k+1$ be defined by

$$R_{L,k+1} = \frac{1}{2}(L_{k+1} + L_k). \tag{6.2}$$

Whereas $L_{k+1}$ vanishes at the $k+1$ Gauss points, $R_{L,k+1}$ vanishes at the $k+1$ left Radau points. At the boundaries,

$$R_{L,k+1}(-1) = 0 \quad \text{and} \quad R_{L,k+1}(1) = 1. \tag{6.3a,b}$$

Since both $L_k$ and $L_{k+1}$ are orthogonal to $\boldsymbol{P}_{k-1}$, $R_{L,k+1}$ also possesses this property. Equivalently,

$$\mathcal{P}_{k-1}(R_{L,k+1}) = 0. \tag{6.4}$$

Equations (6.3) and (6.4) above imply that $R_{L,k+1}$ is the correction function $g_{R,DG}$. Thus, by (4.10) and (3.8),

$$R_{L,k+1}{}' = \delta_{R,k} = \sum_{m=0}^{k} \frac{2i+1}{2} L_i. \tag{6.5}$$

In a similar manner, the right Radau polynomial of degree $k+1$ is defined by

$$R_{R,k+1} = \frac{(-1)^{k+1}}{2}(L_{k+1} - L_k). \tag{6.6}$$

Then $R_{R,k+1}$ vanishes at the $k+1$ right Radau points. In addition,

$$R_{R,k+1}(-1) = 1, \quad R_{R,k+1}(1) = 0, \tag{6.7a,b}$$

and

$$\mathcal{P}_{k-1}(R_{R,k+1}) = 0. \tag{6.8}$$

Properties (6.7) and (6.8) above imply that $R_{R,k+1}$ is the correction function $g_{L,\text{DG}}$. By (4.15) and (3.8),

$$R_{R,k+1}' = -\delta_{L,k} = -\sum_{m=0}^{k} \frac{2i+1}{2}(-1)^i L_i. \tag{6.9}$$

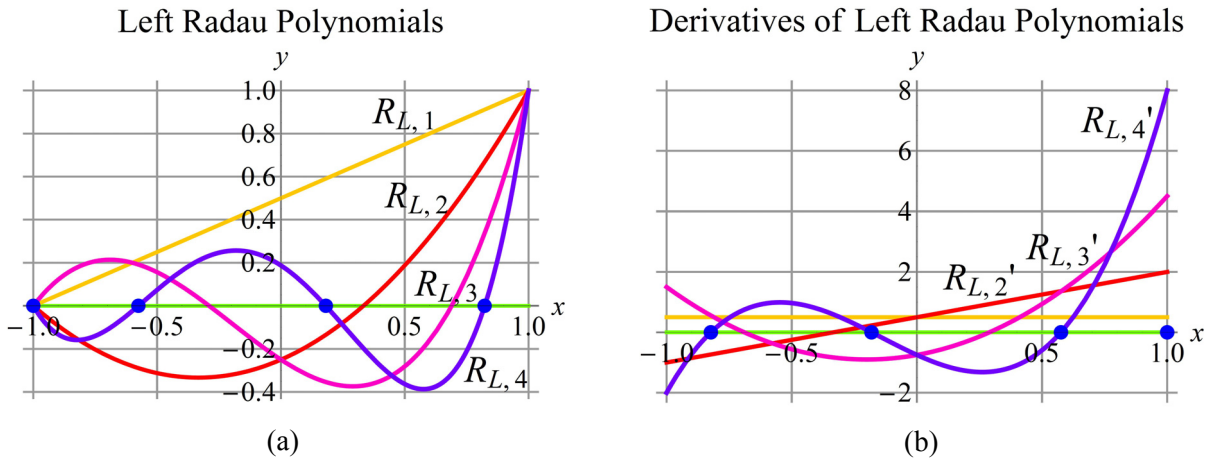The plots of the first few left and right Radau polynomials and their derivatives are shown in Figures 6.1 and 6.2.



Figure 6.1.—(a) Graphs of the left Radau polynomials $R_{L,k}$, $k \le 4$ (the dots are the 4 left Radau points) and (b) their derivatives. The $k-1$ zeros of $R_{L,k}'$ together with $x = 1$ form the $k$ right Radau points.
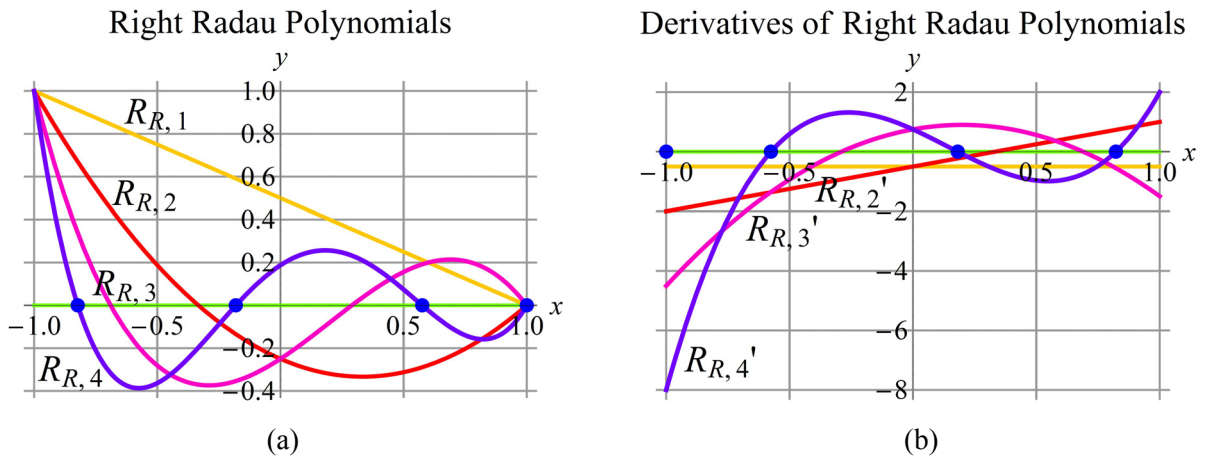


Figure 6.2.—Graphs of (a) the right Radau polynomials $R_{R,k}$, $k \le 4$ (the dots are the 4 right Radau points) and (b) their derivatives. The $k-1$ zeros of $R_{R,k}'$ together with $x = -1$ form the $k$ left Radau points.

**Lobatto polynomials.** For any integer $k \ge 2$, let the Lobatto polynomial of degree $k$ be defined by

$$\mathrm{Lo}_k = L_k - L_{k-2}. \tag{6.10}$$

Then

$$\mathrm{Lo}_k(-1) = \mathrm{Lo}_k(1) = 0. \tag{6.11}$$

and, by definition (6.4), $\mathrm{Lo}_k$ is orthogonal to $\boldsymbol{P}_{k-3}$. The zeros of the Lobatto polynomial of degree $k$ are the $k$ Lobatto points; they include the two boundaries $\pm 1$. The derivative of $\mathrm{Lo}_{k+1}$, which has not been employed by FR authors and play an important role here, is given by

$$\mathrm{Lo}_{k+1}' = (2k + 1)L_k. \tag{6.12}$$

The plots of the Lobatto polynomials $\mathrm{Lo}_k$, $k = 1, \dots, 4$, and their derivatives are shown in Figure 6.3.

**6.2. FR schemes.** Due to symmetry, we focus only on $g_R$ ($g_L$ involves an extra factor $(-1)^k$). For the DG scheme, as discussed after (6.14),

$$g_{R,\mathrm{DG}} = R_{L,k+1}. \tag{6.13}$$

Note that the correction function for the *right* boundary is the *left* Radau polynomial.

The correction functions for the ESFR methods of Section 5 can now be derived. First, for simplicity, denote
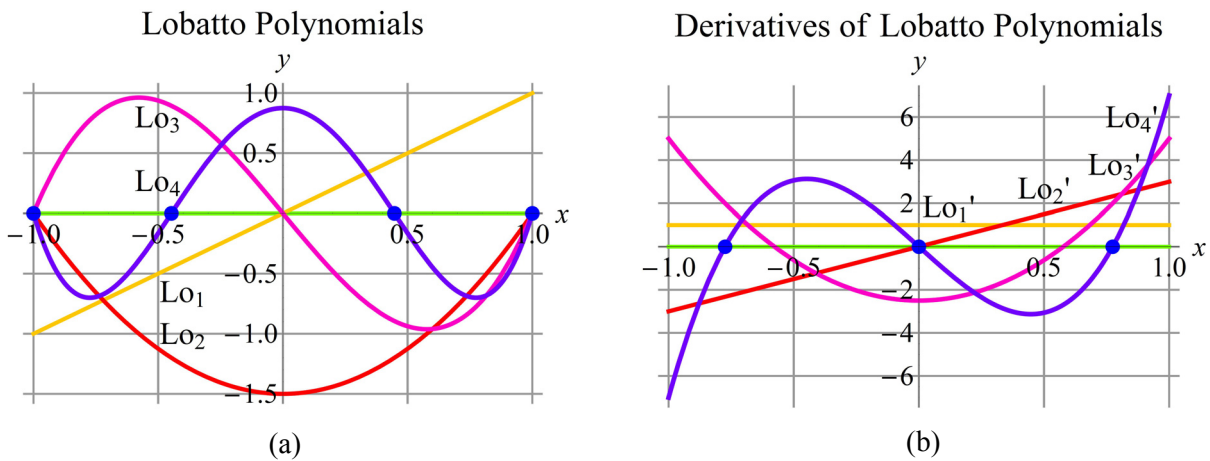
$$g = g_R.$$



Figure 6.3.—Graphs of (a) the Lobatto polynomials $\mathrm{Lo}_k$, $k = 1,\dots,4$ and (b) their derivatives.

Next, $g$ is assumed to satisfy the two conditions (6.1). For the $k$ additional conditions, instead of requiring $g$ to be orthogonal to $\boldsymbol{P}_{k-1}$ as in the case of the DG scheme, we require it to be orthogonal to $\boldsymbol{P}_{k-2}$. It was verified via Fourier analysis (Huynh 2007, 2009) that if $g$ is orthogonal to $\boldsymbol{P}_{k-2}$ the resulting scheme is stable (the converse is not true, however).

Since both $R_{L,k+1}$ and $R_{L,k}$ are orthogonal to $\boldsymbol{P}_{k-2}$, if $g$ orthogonal to $\boldsymbol{P}_{k-2}$, it can be written as

$$g = \alpha R_{L,k+1} + (1 - \alpha) R_{L,k} \tag{6.14}$$

where $\alpha$ remains to be specified (note that the parameter $\alpha$ here is completely independent from the $\alpha$ for the location of the approximate delta function in Section 3). The current author considered only $0 \le \alpha \le 1$ in (Huynh 2009) for the obvious reason that such a correction function is a weighted average of the two Radau polynomials (correction functions). For $\alpha > 1$, the correction function becomes steeper than $g_{DG}$ and, in conjunction with an explicit time stepping method, the largest possible time step size or CFL limit becomes smaller than that for DG, a disadvantage. For $\alpha < 0$ the scheme is unstable. Concerning only energy stability and accuracy, however, $\alpha$ can be larger than 1.

The above implies,

$$g = \alpha\left(R_{L,k+1} - R_{L,k}\right) + R_{L,k} = \frac{\alpha}{2} \text{Lo}_{k+1} + R_{R,k}. \tag{6.15}$$

The second equality is a result of (6.10) and (6.2). Note that $\alpha = 1$ recovers the DG correction function. By (6.12), the above implies

$$g' = \frac{\alpha}{2}(2k+1)L_k + R'_{L,k} = \frac{\alpha}{2}(2k+1)L_k + \delta_{R,k-1}. \tag{6.16}$$

Thus, by (5.10), we obtain the ESFR methods with

$$\alpha_k = \frac{\alpha}{2}(2k+1), \tag{6.17}$$

and the method is energy stable if $\alpha > 0$.

Concerning accuracy, it was found by experiments using Fourier analyses (Huynh 2007) that if $g$ is orthogonal to $\boldsymbol{P}_m$, then resulting scheme is accurate to order $k + m + 2$. Using this criteria, the DG scheme is accurate to order $2k + 1$, and the schemes of the ESFR family, order $2k$. The expected order of accuracy is $k + 1$. Due to this higher than expected accuracy, these methods are said to be super-accurate or to possess the property of super-convergence.

Next, noteworthy members of the one parameter family of correction functions (6.14) are discussed.

The first choice for $g$ is (6.13), which results in the DG scheme.

The second choice for $g$, denoted by $g_2$ or $g_{\text{Lump,Lo}}$ (for 'lumping for Lobatto points'), is defined as follows. Since a steeper correction function tends to result in a scheme with a smaller CFL limit, to make $g$ less steep, the extra condition is obtained by pushing one of the zeros to the left boundary, i.e., $\xi = -1$ is a zero of multiplicity two. After some algebra (Huynh 2007),

$$g_2 = g_{\text{Lump,Lo}} = \frac{k}{2k+1} R_{L,k+1} + \frac{k+1}{2k+1} R_{L,k}.$$

The function $g_2$ has the following remarkable property. Among the $k+1$ Lobatto points (and we can use them as solution points), $g_2'$ vanishes at $k$ of them; the exception is the right boundary where the right flux jump locates.

The final choice here for $g$ requires that $g$ vanishes at the $k$ Gauss points (Huynh2007),

$$g_{\mathrm{Ga}} = \frac{k+1}{2k+1} R_{L,k+1} + \frac{k}{2k+1} R_{L,k}.$$

Whereas the staggered-grid (Kopriva and Kolias 1996) and SD schemes are mildly unstable, the above provides a modification using the $k$ Gauss points as flux points. The resulting scheme is both Fourier and energy stable for all $k$.

Also note that the steepest slope of $g$, which takes place at the right boundary, relates to the time step size or CFL limit. For example, for DG, $g' = R'_{L,k+1}(1) = (k+1)^2/2$; when an explicit Runge-Kutta method is employed, it is well known that the CFL limit for the DG scheme of degree $k$ is roughly proportional to $1/k^2$.

As an example of correction functions, Fig. 6.4(a) shows the plots of the functions $g_{\mathrm{DG}}$, $g_{\mathrm{Ga}}$, and $g_2$ for $k = 3$. Figure 6.4(b) shows the (top half of) spectra of the corresponding schemes. Note that all three methods are stable since the spectra lie in the left half of the complex plane. The spectra intersect the real axis at $x_{\mathrm{DG}} = -19.2$, $x_{\mathrm{Ga}} = -12.3$, and $x_2 = -9.6$. If the RK4 method is employed for time stepping, then the CFL limits are approximately .145, .227, and .289, respectively.

Table 1 tabulates the orders of accuracy and errors of these semi-discrete schemes for $k = 3$. Here, the coarse mesh error corresponds to $w = \pi/4$, and fine mesh error, $w = \pi/8$ so that errors are away from machine zero, and the calculation of order of accuracy is valid.

Note that for each $k$, all errors have negative real parts—a fact consistent with the stability of the three schemes. In addition, the dominant part of the error for the DG scheme is real (dissipation type) whereas those for the other two schemes are imaginary (dispersion type).
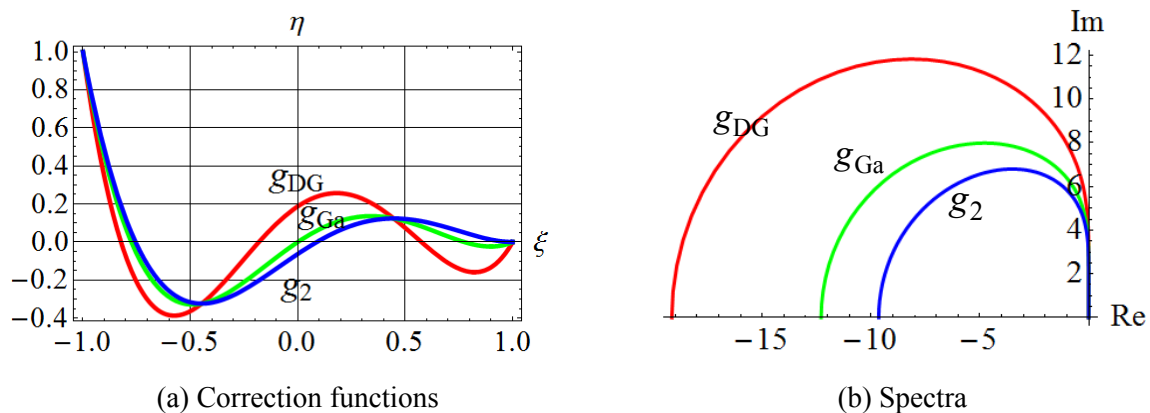


(a) Correction functions        (b) Spectra

Figure 6.4.—(a) Correction functions for $k$ = 3, and (b) their spectra.

TABLE 1.—ORDERS OF ACCURACY AND ERRORS OF SCHEMES FOR $k = 3$

| Scheme | Order of accuracy | Coarse mesh error, $w = \pi/4$ | Fine mesh error, $w = \pi/8$ |
|---|---|---|---|
| DG | 7 | $-1.\times10^{-7}-1.\times10^{-8}i$ | $-4.\times10^{-10}-2.\times10^{-11}i$ |
| $g_{Ga}$ | 6 | $-3.1\times10^{-7}+1.3\times10^{-6}i$ | $-1.2\times10^{-9}+1.1\times10^{-8}i$ |
| $g_2$ | 6 | $-5.4\times10^{-7}+2.3\times10^{-6}i$ | $-2.2\times10^{-9}+1.9\times10^{-8}i$ |

A brief review of Fourier analysis for these type of methods can be found in the Appendix.

Concerning open problems, it remains to be shown whether Fourier stability is equivalent to energy stability.

Also note that there exists correction functions that are not orthogonal to any $\boldsymbol{P}_m$, but the resulting scheme is Fourier stable. As an example, the correction function $g_R$ that lumps all corrections to the right boundary when the solution points are the Chebyshev-Lobatto points (Huynh 2007) possesses this property. It remains an open problem to identify all correction functions that yields stable schemes.

# 7. Conclusions and Discussion

In conclusion, a formulation for the discontinuous Galerkin (DG) method that leads to solutions using the differential form of the equation was presented. The formulation includes (a) a derivative calculation that involves only data within each cell with no data interaction among cells, and (b) for each cell, corrections to this derivative that deal with the jumps in fluxes at the cell boundaries and allow data across cells to interact. The derivative with no interaction is obtained by projection or interpolation, and the corrections are derived using the approximate (Dirac) delta functions. The formulation results in a family of schemes: different approximate delta functions give rise to different methods. It was shown that the current formulation is equivalent to the flux reconstruction (FR) formulation. Due to the use of approximate delta functions, an energy stability proof simpler than that of Vincent, Castonguay, and Jameson (2011) for a family of schemes was derived. Accuracy and stability of resulting schemes were examined via Fourier analyses. Some open problems were discussed. The current and FR formulations appear to be promising toward the goal of faster and more accurate solutions of conservation laws for practical applications.

# Appendix—A Brief Review of Fourier Stability and Accuracy Analysis

Accuracy and stability of a numerical method are critical and can be derived via Fourier analyses. On $(-\infty, \infty)$, consider the advection equation

$$u_t + u_x = 0. \tag{A.1}$$

The initial condition at $t = 0$ is periodic: $u_{\text{init}} = e^{Iwx}$ where $w$ is a real number between $-\pi$ and $\pi$ called a wave number and, in this section, $I = \sqrt{-1}$. Low frequency data corresponds to $w$ of small magnitude, high frequency, to $w$ near $\pm\pi$. The exact solution is $u_{\text{exact}}(x, t) = e^{Iw(x-t)}$. At $x = 0$ and $t = 0$,

$$(u_{\text{exact}})_t(0, 0) = -Iw. \tag{A.2}$$

The cells are $E_j = [j - 1/2, j + 1/2]$. At time $t = 0$, the data $u_{\text{init}}$ on $E_j$ is $e^{Iw(j+\xi/2)}$ where $|\xi| \le 1$. Thus, the exact data on $E_{j-1}$ is

$$e^{-Iw}e^{Iw(j+\xi/2)}.$$

In the local description, $u_j(\xi) = \sum_{i=0}^{k} u_{j,i} L_i(\xi)$. For the calculation of eigenvalues below, we assume the data share the above property with the exact solution: $u_{j-1}(\xi) = e^{-Iw}u_j(\xi)$, or, for all $i$, $0 \le i \le k$,

$$u_{j-1,i} = e^{-Iw}u_{j,i}. \tag{A.3}$$

To calculate the eigenvalues, the $k + 1$ values $u_{j,i}$ are grouped together as a vector: with superscript $T$ denoting the transpose, set

$$\boldsymbol{u}_j = \left(u_{j,0}, \ldots, u_{j,k}\right)^T. \tag{A.4}$$

The solution of (A.1) by the methods of the previous sections on each cell $E_j$ can be expressed as

$$\frac{d}{dt}\boldsymbol{u}_j = \boldsymbol{C}_{-1}\boldsymbol{u}_{j-1} + \boldsymbol{C}_0\boldsymbol{u}_j \tag{A.5}$$

where $\boldsymbol{C}_{-1}$ and $\boldsymbol{C}_0$ are $(k + 1) \times (k + 1)$ matrices. Using (A.3), we replace $\boldsymbol{u}_{j-1}$ by $e^{-Iw}\boldsymbol{u}_j$. The spatial discretization results in

$$\frac{d}{dt}\boldsymbol{u}_j = \boldsymbol{S}\boldsymbol{u}_j \tag{A.6}$$

where the $(k + 1) \times (k + 1)$ matrix $\boldsymbol{S}$ (for 'space' or 'semi-discrete') is given by

$$\boldsymbol{S} = e^{-Iw}\boldsymbol{C}_{-1} + \boldsymbol{C}_0. \tag{A.7}$$

Equation (A.6) is similar to the differential equation $du/dt = \lambda u$ whose solution is $ce^{\lambda t}$ where $c$ is an arbitrary constant. If $\text{Re}(\lambda) \le 0$, the solution is stable. Here, the eigenvalues of $\boldsymbol{S}$ take the place of $\lambda$. For all schemes discussed here, $\boldsymbol{S}$ has $k + 1$ eigenvalues. Among these, the *principal eigenvalue*, denoted by $S(w)$, is the one approximating the exact value $-Iw$ of (A.2). All eigenvalues must lie in the left half of the complex plane for the semi-discretization to be stable. The collection of all eigenvalues forms the *spectrum* of the scheme.

To find the order of accuracy, note that with a uniform mesh of width $h$, the principal eigenvalue $S(w)$ 'approximates' $-h\partial/\partial x$. A scheme is accurate to order $m$ if $S$ 'approximates' $-h\partial/\partial x$ to $O(h^{m+1})$; more precisely, for small $w$,

$$S(w) = -Iw + O(w^{m+1}). \tag{A.8}$$

In practice, we obtain the order of accuracy of a scheme by the following procedure. First, set $w$ to be, say, $\pi/4$. We can estimate the error

$$E(w) = S(w) + Iw \tag{A.9}$$

By halving the wave number $w$ (which is equivalent to doubling the number of mesh points), the error corresponding to $w/2\ (=\pi/8)$ is

$$E(w/2) = S(w/2) + Iw/2. \tag{A.10}$$

Since $O((w/2)^{m+1}) \approx (1/2)^{m+1}O((w)^{m+1})$, for a scheme to be $m$-th order accurate, the following condition must hold: $E(w)/E(w/2) \approx 2^{m+1}$. That is, the order of accuracy is given by

$$m \approx \text{Log}\left(\frac{E(w)}{E(w/2)}\right)/\text{Log}(2) - 1. \tag{A.11}$$

# References

Y. Allaneau and A. Jameson (2011), Connections between the filtered discontinuous Galerkin method and the flux reconstruction approach to high order discretizations, Comput. Methods Appl. Mech. Engrg., 200 (2011) 3628–3636

F. Bassi and S. Rebay (1997a), A high-order accurate discontinuous finite element method for the numerical solution of the compressible Navier-Stokes equations, J. Comput. Phys., 131 (1997), pp. 267-279.

F. Bassi and S. Rebay (1997b), High-order accurate discontinuous finite element solution for the 2D Euler equations, J. Comput. Phys., 138, pp. 251-285.

F. Bassi and S. Rebay (2000), A high order discontinuous Galerkin method for compressible turbulent flows, in "Discontinuous Galerkin methods: Theory, Computation, and Application", B. Cockburn, G. Karniadakis, and C.-W. Shu, editors, Lecture Notes in Computational Science and Engineering, Springer, pp. 77-88.

P. Castonguay, P. E. Vincent, A. Jameson (2012), A New Class of High-Order Energy Stable Flux Reconstruction Schemes for Triangular Elements, Journal of Scientific Computing, Volume 51, Number 1, Pages 224-256.

P. Castonguay, D. M. Williams, P. E. Vincent, A. Jameson (2013), Energy Stable Flux Reconstruction Schemes for Advection-Diffusion Problems. P. Computer Methods in Applied Mechanics and Engineering. Under Review.

B. Cockburn, G. Karniadakis, and C.-W. Shu, Eds., (2000), Discontinuous Galerkin methods: Theory, Computation, and Application (Springer).

B. Cockburn and C.-W. Shu (1998), The local discontinuous Galerkin methods for time-dependent convection diffusion systems, SIAM J. Numer. Anal., 35, pp. 2440-2463

B. Cockburn and C.-W. Shu (2005), Foreword for the special issue on discontinuous Galerkin method, Journal of Scientific Computing, 22-23, pp. 1–3.

B. Cockburn and C.-W. Shu (2009), Foreword for the special issue on discontinuous Galerkin method, Journal of Scientific Computing, 40, pp. 1–3.

H. Gao and Z.J. Wang (2009), A High-Order Lifting Collocation Penalty Formulation for the Navier-Stokes Equations on 2-D Mixed Grids, AIAA-2009-3784.

H. Gao and Z.J. Wang (2013), A Conservative Correction Procedure via Reconstruction Formulation with the Chain-Rule Divergence Evaluation", J. Computational Physics 232, 7–13.

H. Gao, Z.J. Wang, and H. T. Huynh (2013), Differential Formulation of Discontinuous Galerkin and Related Methods for the Navier-Stokes Equations, Commun. Comput. Phys, Vol. 13, No. 4, pp. 1013-1044.

T. Haga, H. Gao, Z.J. Wang (2010), A High-Order Unifying Discontinuous Formulation for 3-D Mixed Grids, AIAA Paper 2010-540.

T. Haga, H. Gao and Z. J. Wang (2011), A High-Order Unifying Discontinuous Formulation for the Navier-Stokes Equations on 3D Mixed Grids, Math. Model. Nat. Phenom., Vol. 6 (3), 28-56.

J.S. Hesthaven and Tim Warburton (2008), *Nodal Discontinuous Galerkin Methods* (Springer).

F.B. Hildebrand (1987), Introduction to Numerical Analysis, Second Edition, Dover Books on Advanced Mathematics.

H.T. Huynh (2007), A flux reconstruction approach to high-order schemes including discontinuous Galerkin methods, AIAA Paper 2007-4079.

H.T. Huynh (2009), A Reconstruction Approach to High-Order Schemes Including Discontinuous Galerkin for Diffusion, AIAA Paper 2009-403.

H.T. Huynh, Z. J. Wang, and P. E. Vincent (2014), High-order methods for computational fluid dynamics: A brief review of compact differential formulations on unstructured grids, Computers and Fluids, to appear.

A. Jameson (2010), A proof of the stability of the spectral difference method for all orders of accuracy, J. Sci. Comput. 45(1–3), 348–358.

A. Jameson, P. E. Vincent, P. Castonguay (2012), On the Non-Linear Stability of Flux Reconstruction Schemes, Journal of Scientific Computing, Volume 50, Number 2, Pages 434-445

G. Jiang and C.-W. Shu (1994), On cell entropy inequality for discontinuous Galerkin methods, Math. Comp., Vol. 62, Number 206, pp. 531-538.

D.A. Kopriva and J.H. Kolias (1996), A conservative staggered-grid Chebyshev multidomain method for compressible flows, J. Comput. Phys. 125, 244.

P. LaSaint and P.A. Raviart (1974), On a finite element method for solving the neutron transport equation, in Mathematical aspects of finite elements in partial differential equations, C. de Boor (ed.), Academic Press, pp. 89–145.

C. Liang, A. Jameson, Z.J. Wang (2009a), Spectral difference method for compressible flow on unstructured grids with mixed elements. J. Comput. Phys. 228, 2847.

C. Liang, S. Premasuthan, A. Jameson (2009b), High-order accurate simulation of low-Mach laminar flow past two side-by-side cylinders using spectral difference method. Comput. Struct. 87, 812.

Y. Liu, M. Vinokur, and Z.J. Wang (2006), Discontinuous Spectral Difference Method for Conservation Laws on Unstructured Grids, J. Comput. Phys., 216, 780–801.

P.M. Morse and H. Feshbach, Methods of Theoretical Physics, Vol. 1, McGraw-Hill, New York, 1953.

S. Osher (1984), Riemann solvers, the entropy condition, and difference approximations, SIAM J. Numer. Anal. Vol. 21, No 2, 217-235.

W.H. Reed and T.R. Hill (1973), Triangular mesh methods for the neutron transport equation, Los Alamos Scientific Laboratory Report, LA-UR-73-479.

C.-W. Shu (2012), Discontinuous Galerkin method for time dependent problems: survey and recent developments. Preprint.

P.E. Vincent, P. Castonguay, A. Jameson (2011a), A New Class of High-Order Energy Stable Flux Reconstruction Schemes, Journal of Scientific Computing, Volume 47, Number 1, Pages 50-72.

P.E. Vincent, P. Castonguay, A. Jameson (2011b), Insights from von Neumann Analysis of High-Order Flux Reconstruction Schemes, J. Comput. Phys., Vol. 230, Issue 22, pp. 8134-8154.

Z.J. Wang (2007), High-order methods for the Euler and Navier-Stokes equations on unstructured grids, Journal of Progress in Aerospace Sciences, Vol. 43, pp. 1–41.

Z.J. Wang (2011), Adaptive High-order methods in Computational Fluid Dynamics, Advances in Computational Fluid Dynamics Vol. 2, World Scientific Publishing Co.

Z.J. Wang et al. (2013), High-Order CFD Methods: Current Status and Perspective, Int. J. Numer. Meth. Fluids, 72, No. 8, pp. 811–845.

Z.J. Wang and H. Gao (2009), A Unifying Lifting Collocation Penalty formulation including the discontinuous Galerkin, spectral volume/difference methods for conservation laws on mixed grids, J. Comput. Phys., 228, No. 2, pp. 8161–8186.

Z.J. Wang, H. Gao and T. Haga (2011). A Unifying Discontinuous Formulation for Hybrid Meshes, in Adaptive High-Order Methods in Computational Fluid Dynamics, World Scientific, edited by Z.J. Wang.

Z.J. Wang, Y. Liu, G. May, A. Jameson (2007), Spectral difference method for unstructured grids II: extension to the Euler equations. J. Sci. Comput. 32, 45

Z.J. Wang, L. Zhang and Y. Liu (2004), Spectral (finite) volume method for conservation laws on unstructured grids IV: extension to two-dimensional Euler equations, J. Comput. Phys., 194, No. 2, pp. 716–741.

D.M. Williams, P. Castonguay, P. E. Vincent, A. Jameson (2011), An Extension of Energy Stable Flux Reconstruction to Unsteady, Non-linear, Viscous Problems on Mixed Grids, AIAA Paper 2011-3405.

D.M. Williams, P. Castonguay, P. E. Vincent, A. Jameson (2013), Energy Stable Flux Reconstruction Schemes for Advection-Diffusion Problems on Triangles, Journal of Computational Physics, Under Review.

M. Yu, Z. J. Wang, and H. Hu (2012), High-Fidelity Flapping-Wing Aerodynamics Simulations with a Dynamic Unstructured Grid Based Spectral Difference Method, in Proceedings of the 7th International Conference on Computational Fluid Dynamics, ICCFD7-4104.

| 1. REPORT DATE (DD-MM-YYYY) <br> 01-06-2014 | 2. REPORT TYPE <br> Technical Memorandum | 3. DATES COVERED (From - To) |
|---|---|---|

| 4. TITLE AND SUBTITLE <br> On Formulations of Discontinuous Galerkin and Related Methods for Conservation Laws | 5a. CONTRACT NUMBER |
|---|---|
| | 5b. GRANT NUMBER |
| | 5c. PROGRAM ELEMENT NUMBER |
| 6. AUTHOR(S) <br> Huynh, H., T. | 5d. PROJECT NUMBER |
| | 5e. TASK NUMBER |
| | 5f. WORK UNIT NUMBER <br> WBS 794072.02.03.02.03 |

| 7. PERFORMING ORGANIZATION NAME(S) AND ADDRESS(ES) <br> National Aeronautics and Space Administration <br> John H. Glenn Research Center at Lewis Field <br> Cleveland, Ohio 44135-3191 | 8. PERFORMING ORGANIZATION REPORT NUMBER <br> E-18938 |
|---|---|

| 9. SPONSORING/MONITORING AGENCY NAME(S) AND ADDRESS(ES) <br> National Aeronautics and Space Administration <br> Washington, DC 20546-0001 | 10. SPONSORING/MONITOR'S ACRONYM(S) <br> NASA |
|---|---|
| | 11. SPONSORING/MONITORING REPORT NUMBER <br> NASA/TM-2014-218135 |

**12. DISTRIBUTION/AVAILABILITY STATEMENT**
Unclassified-Unlimited
Subject Category: 59
Available electronically at http://www.sti.nasa.gov
This publication is available from the NASA Center for AeroSpace Information, 443-757-5802

**13. SUPPLEMENTARY NOTES**

**14. ABSTRACT**
A formulation for the discontinuous Galerkin (DG) method that leads to solutions using the differential form of the equation (as opposed to the standard integral form) is presented. The formulation includes (a) a derivative calculation that involves only data within each cell with no data interaction among cells, and (b) for each cell, corrections to this derivative that deal with the jumps in fluxes at the cell boundaries and allow data across cells to interact. The derivative with no interaction is obtained by a projection, but for nodal-type methods, evaluating this derivative by interpolation at the nodal points is more economical. The corrections are derived using the approximate (Dirac) delta functions. The formulation results in a family of schemes: different approximate delta functions give rise to different methods. It is shown that the current formulation is essentially equivalent to the flux reconstruction (FR) formulation. Due to the use of approximate delta functions, an energy stability proof simpler than that of Vincent, Castonguay, and Jameson (2011) for a family of schemes is derived. Accuracy and stability of resulting schemes are discussed via Fourier analyses. Similar to FR, the current formulation provides a unifying framework for high-order methods by recovering the DG, spectral difference (SD), and spectral volume (SV) schemes. It also yields stable, accurate, and economical methods.

**15. SUBJECT TERMS**
Discontinuous Galerkin; High-order methods; Conservation laws; Flux reconstruction

| 16. SECURITY CLASSIFICATION OF: | | | 17. LIMITATION OF ABSTRACT | 18. NUMBER OF PAGES | 19a. NAME OF RESPONSIBLE PERSON <br> STI Help Desk (email:help@sti.nasa.gov) |
|---|---|---|---|---|---|
| a. REPORT <br> U | b. ABSTRACT <br> U | c. THIS PAGE <br> U | UU | 36 | 19b. TELEPHONE NUMBER (include area code) <br> 443-757-5802 |